


ORIGINAL ARTICLE

Integrative genome-wide analyses reveal the transcriptional aberrations in Japanese esophageal squamous cell carcinoma

Akira Takemoto¹ | Kousuke Tanimoto^{2,3}  | Seiichi Mori⁴ | Jun Inoue⁵ | Naoto Fujiwara⁶ | Tetsuo Noda⁷ | Johji Inazawa^{1,5} 

¹Bioresource Research Center, Tokyo Medical and Dental University (TMDU) Yushima, Tokyo, Japan

²Genome Laboratory, Medical Research Institute, TMDU, Tokyo, Japan

³Genomics Research Support Unit, Research Core, TMDU, Tokyo, Japan

⁴Division of Cancer Genomics, Cancer Institute, Japanese Foundation for Cancer Research (JFCR), Tokyo, Japan

⁵Department of Molecular Cytogenetics, Medical Research Institute, TMDU, Tokyo, Japan

⁶Department of Gastrointestinal Surgery, TMDU, Tokyo, Japan

⁷Cancer Institute, Japanese Foundation for Cancer Research (JFCR), Tokyo, Japan

Correspondence

Kousuke Tanimoto and Johji Inazawa, Tokyo Medical and Dental University (TMDU), 1-5-45 Yushima, unkyo-ku, Tokyo, 113-8519, Japan.

Email: ktani.nri@mri.tmd.ac.jp (K. T.) and johinaz.cgen@mri.tmd.ac.jp (J. I.)

Funding information

Grants-in-Aid for Scientific Research, Grant/Award Number: 16K14630; Conquering cancer through NEO-dimensional systems understandings, Grant/Award Number: 15H05908; Japan Agency for Medical Research and Development (AMED); Nanken-Kyoten, TMDU

Abstract

Esophageal squamous cell carcinoma (ESCC) is a malignant disease. At present, the genomic profiles of ESCC are known to a considerable extent, and DNA methylation and gene expression profiles have been mainly used for the classification of ESCC subtypes, but integrative genomic, transcriptomic, and epigenomic analyses remain insufficient. Therefore, we performed integrative analyses using whole-exome sequencing, DNA methylation, and RNA sequencing (RNA-seq) analyses of Japanese patients with ESCC. In cancer-related genes, such as NOTCH family genes, RTK/PI3K pathway genes, and NFE2L2 pathway genes, variants and copy number amplification were detected frequently. Japanese ESCC cases were clustered into two mutational signatures: an APOBEC-associated signature and an age-related signature. In imprinted genes, DNA methylation was aberrant in gene promoter regions and correlated well with gene expression profiles. Nonsynonymous single-nucleotide variants and allelic expression imbalance were detected frequently in FAT family genes. Our integrative genome-wide analyses, including DNA methylation and allele-specific gene expression profiles, revealed altered gene regulation of imprinted genes and FAT family genes in ESCC.

KEYWORDS

allelic expression imbalance, DNA methylation, esophageal squamous cell carcinoma, imprinted gene, integrative analysis

Akira Takemoto and Kousuke Tanimoto contributed equally to this work.

This is an open access article under the terms of the Creative Commons Attribution-NonCommercial License, which permits use, distribution and reproduction in any medium, provided the original work is properly cited and is not used for commercial purposes.

© 2021 The Authors. *Cancer Science* published by John Wiley & Sons Australia, Ltd on behalf of Japanese Cancer Association.

1 | INTRODUCTION

Esophageal cancer is a well-known malignant disease. It ranks seventh in terms of worldwide incidence and is tenth in Japan.^{1,2} Esophageal cancer is classified into two types: esophageal adenocarcinoma (EAC) or esophageal squamous cell carcinoma (ESCC). In Western countries, EAC is the predominant form of esophageal cancer. In contrast, ESCC is the predominant form in Asia, including Japan. Although there have been advances in surgical techniques and chemotherapy, ESCC remains one of the most fatal cancers.³ Furthermore, effective molecular targeted therapies for ESCC have not been developed yet. Therefore, several genome-wide studies have been performed, and integrated landscapes of genome, epigenome, and gene expression are becoming clear. Somatic variants in *TP53*, *PI3K* pathway genes, *NOTCH* family genes, *FAT* family genes, and oxidative stress response genes, such as *NFE2L2*, have been identified as characteristics of ESCC by several groups of investigators, including The Cancer Genome Atlas (TCGA) Research Network.⁴⁻¹⁰ The genomic profiles of ESCC have been elucidated to a considerable extent, and DNA methylation and gene expression profiles have been mainly used for the classification of ESCC subtypes,⁴⁻¹⁰ but integrative genomic, transcriptomic, and epigenomic analyses remain insufficient.

Therefore, we performed integrated analyses from a viewpoint different from previous studies using whole-exome sequencing (WES), DNA methylation, and RNA-sequencing (RNA-seq) analyses of Japanese patients with ESCC. In this study, in addition to genome analysis, we examined what functions and which pathways are involved in aberrations through DNA methylation status. Furthermore, we revealed allelic expression imbalance (AEI) using RNA-seq data. If the allelic expression of genes harboring nonsynonymous variants is transcribed predominantly from only one allele and little from the paired allele in the tumor, this phenomenon may function as a deleterious mutation to cause altered functions of the corresponding genes. Our study reiterates the possible involvement of AEI and aberrant expression of imprinted genes in the pathogenesis of ESCC, providing a new concept for the development of therapeutic modalities for patients with ESCC.

2 | Materials and methods

2.1 | Sample collection

Tumor samples of ESCC were obtained from two hospitals (68 samples from Tokyo Medical and Dental University [TMDU] Medical Hospital and 20 samples from The Cancer Institute Hospital of

Japanese Foundation for Cancer Research [JFCR]). Clinical information of samples analyzed in this study is shown in Table S1. All samples were fresh-frozen primary resections without previous chemotherapy or radiation. To perform integrative analyses, DNA and RNA used for whole-exome sequencing, DNA methylation analysis, and RNA-seq were extracted from an identical piece of the clinical specimen. Written informed consent was received from all patients, and the study protocol was reviewed and approved by the internal review boards of TMDU and JFCR.

2.2 | Whole-exome sequencing and RNA-seq

DNA extracted from all 88 ESCCs and paired nontumor tissue samples was captured using SureSelect XT Human All Exon (Agilent Technologies), and captured DNA was sequenced by HiSeq2000 (Illumina).

Total RNA was extracted from 57 ESCCs and paired nontumor tissue samples, and mRNA was sequenced by HiSeq2000 (Illumina).

The details of sequencing and data analyses are described in Supplementary Methods.

2.3 | Evaluation of DNA methylation status of imprinted genes

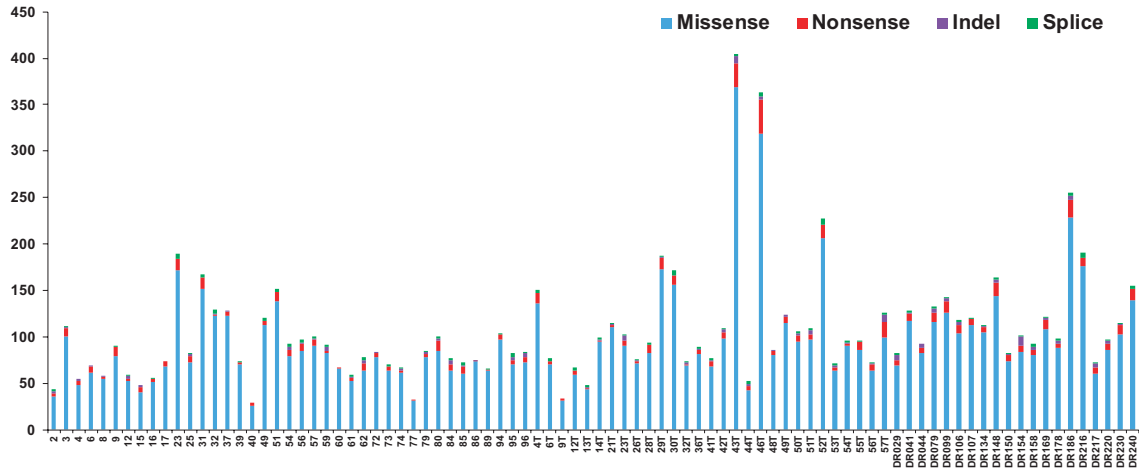
DNA methylation status of imprinted genes was evaluated in 67 samples from TMDU Medical Hospital, which we previously analyzed using Illumina Infinium HumanMethylation450 BeadChip (HM450).¹¹ In this study, we used 144 003 CpG sites located in promoter regions. We used 87 genes as a human imprinted gene set extracted from Babak's study excluding noncoding genes.¹² The details of the analysis are described in Supplementary Methods.

2.4 | Analysis of AEI

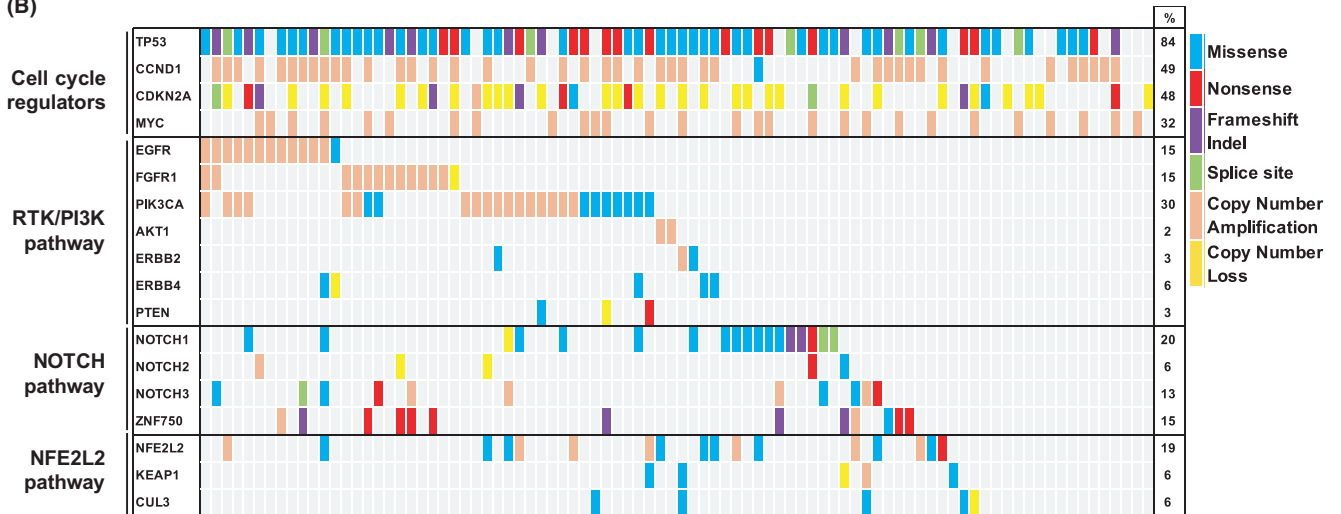
Single nucleotide variant (SNV) calling of aligned sequence reads for RNA-seq was performed for 56 samples having both WES and RNA-seq data from TMDU Medical Hospital by Genome Analysis ToolKit (GATK).¹³ AEI genes were defined as those bearing more than two SNVs that exhibited significant differences in allele frequency in reading transcripts of >30 between tumor and nontumor tissues. We excluded genes coded on chromosomes X and Y in this analysis due to X inactivation in females and frequent somatic loss of Y in cancer.

FIGURE 1 Somatic variants detected by WES in 88 Japanese esophageal squamous cell carcinoma (ESCC) cases. A, The number of detected SNVs and insertions and deletions (indels) (vertical axis) in each sample (horizontal axis). B, The matrix of detected variants colored by the type of variant. Each row represents a gene and each column represents an individual sample. Blue, nonsynonymous SNVs; red, nonsense SNVs; purple, indels; green, splice-site SNVs; beige, copy number amplification; yellow, copy number loss. C, Copy number profiles analyzed by GISTIC2 across 88 ESCC samples. The left and right panels indicate the profiles of copy number amplification and copy number loss, respectively

(A)



(B)



(C)

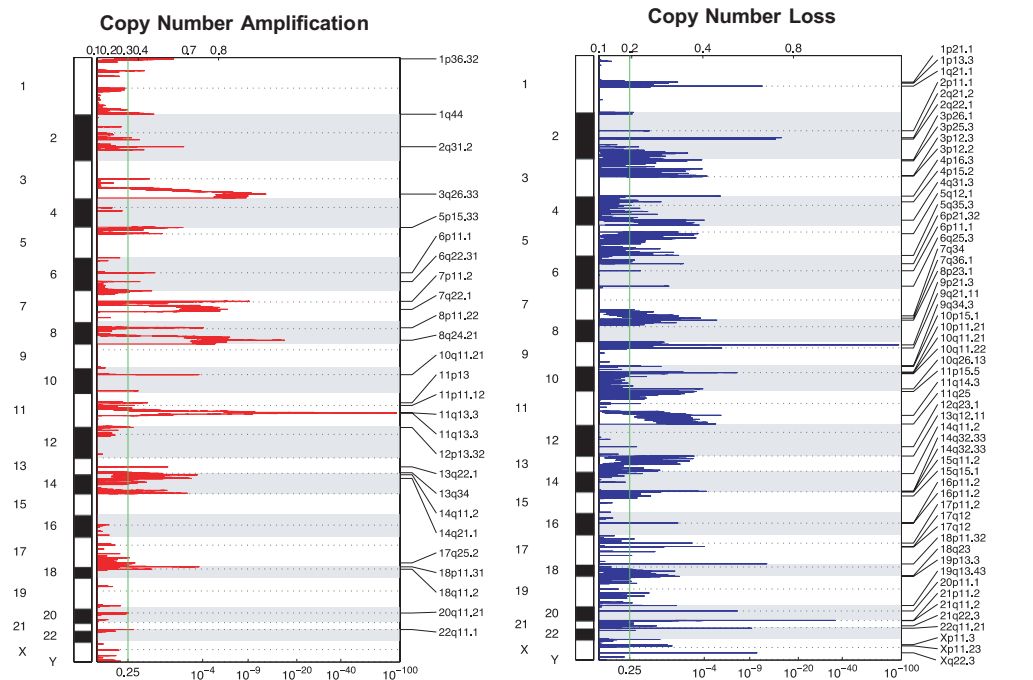


TABLE 1 Frequently amplified genes identified by GISTIC analysis

Gene	Cytoband	Number of samples
FGF3	11q13.3	50
ANO1	11q13.3	49
FADD	11q13.3	49
PPFIA1	11q13.3	49
CTTN	11q13.3	49
SHANK2	11q13.3	47
FGF19	11q13.3	45
FGF4	11q13.3	45
CCND1	11q13.3	43
ORAOV1	11q13.3	43
TPCN2	11q13.3	39
MYEOV	11q13.3	39
MRGPRF	11q13.3	31
PVT1	8q24.21	30
IGHMBP2	11q13.3	30
MRGPRD	11q13.3	30
ATP11B	3q26.33	28
PCAT1	8q24.21	28
PRNCR1	8q24.21	28
CCAT1	8q24.21	28
CCAT2	8q24.21	28
POU5F1B	8q24.21	28
MYC	8q24.21	28

2.5 | Data visualization

The protein schematics were visualized using ProteinPaint (<https://proteinpaint.stjude.org/>).¹⁴ Sequence read data were visualized using Integrated Genomics Viewer (IGV).¹⁵⁻¹⁷

3 | Results

3.1 | Somatic variants and copy number alterations in Japanese ESCC samples

Tumor and paired nontumor DNA from 88 Japanese patients with ESCC was subjected to WES. The details of sequencing statistics for WES are shown in Table S1. Nonsynonymous somatic variants (NSVs), defined as SNVs, splice sites that are flanking regions of exon-intron

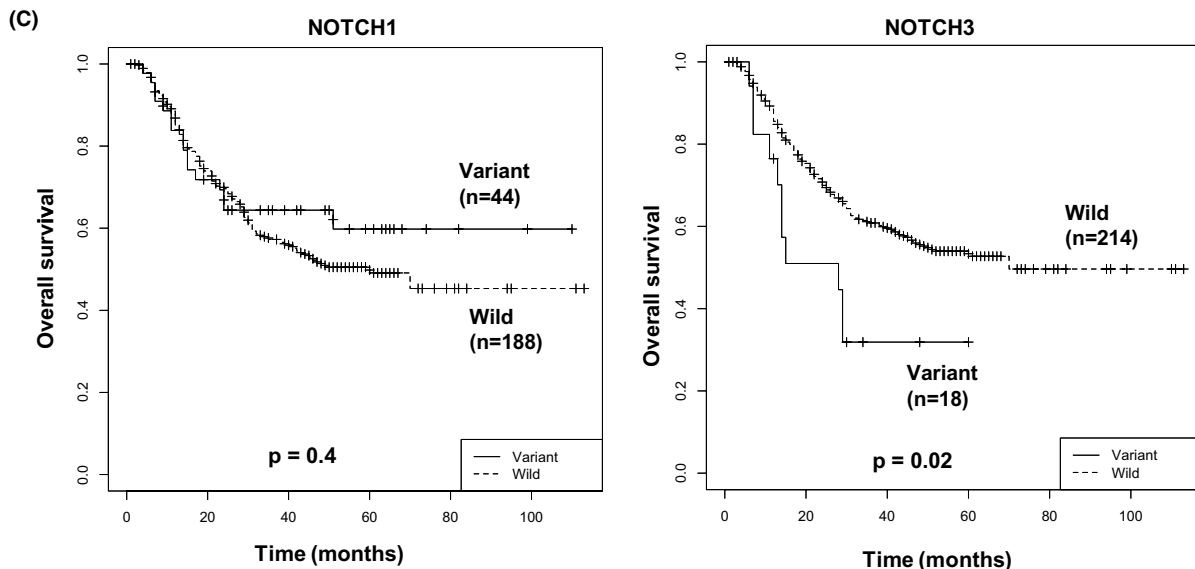
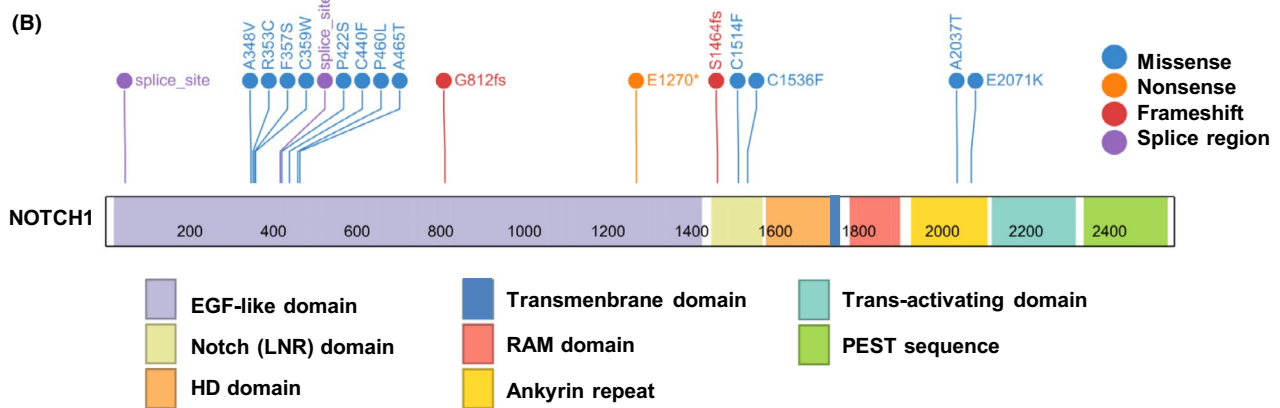
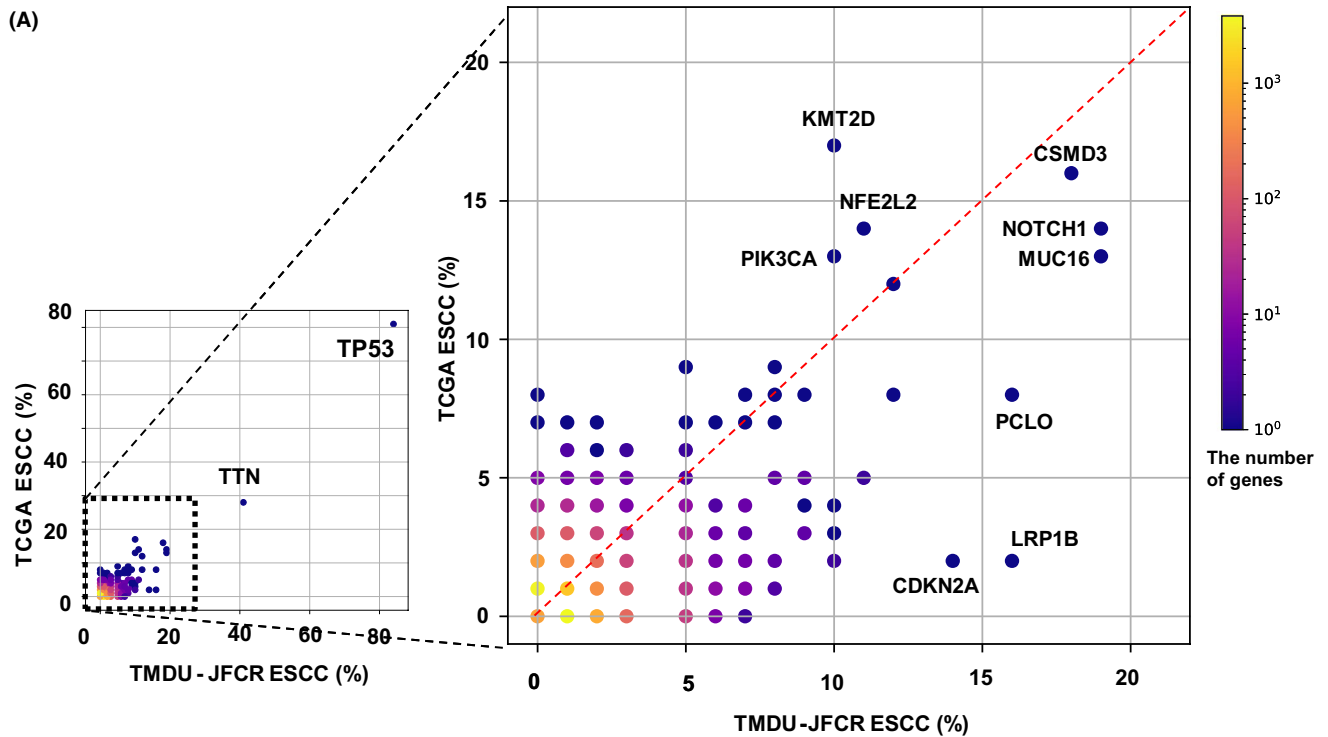
TABLE 2 Frequently deleted genes identified by GISTIC analysis

Gene	Cytoband	Number of samples
CDKN2A	9p21.3	30
MTAP	9p21.3	27
C9orf53	9p21.3	27
CDKN2B	9p21.3	27
DMRTA1	9p21.3	20
ELAVL2	9p21.3	12
LRP1B	2q22.1	11
IFNE	9p21.3	8
ROCK1P1	18p11.32	8
CIDECP	3p25.3	7
FBXW7	4q31.3	7
DEFB103A	8p23.1	7
DEFB103B	8p23.1	7
DEFB109P1B	8p23.1	7
DEFB4B	8p23.1	7
FAM66B	8p23.1	7
SPAG11B	8p23.1	7
USP17L1P	8p23.1	7
USP17L4	8p23.1	7
ZNF705G	8p23.1	7
IFNA1	9p21.3	7

junctions and frameshift insertions and deletions (indels) in this study, and copy number alterations were detected by the procedures described in the Materials and Methods section. A total of 9301 variants were identified, of which 9138 were single-nucleotide alterations and 163 were frameshift indels. The mean number of variants was 105 (range of 29-405). The number of variants in each sample was plotted in Figure 1A, and the details of variants are shown in Table S2. The most frequently NSV-detected gene was *TP53* (74/88, 84%), followed by *TTN* (41%), *NOTCH1* (19%), *MUC16* (19%), *CSMD3* (18%), *LRP1B* (16%), *PCLO* (16%), *CDKN2A* (14%), *HYDIN* (13%), *ZNF750* (13%), *NFE2L2* (11%), *SYNE1* (11%), and *MUC4* (11%).

Exome-based copy number profiling was performed by GISTIC2. NSVs and copy number alterations in genes involved in the RTK/PI3K pathway, NOTCH family, and NFE2L2 pathway were detected in a mutually exclusive manner (Figure 1B). Copy number profiles analyzed by GISTIC2 across 88 ESCC samples were plotted in Figure 1C. Copy number alteration status of all genes is shown in Table S3. Copy number amplifications were frequently found at four hotspot regions: 11q13.3(57%, 50/88), 8q24.21(34%, 30/88),

FIGURE 2 Somatic variants in NOTCH1. A, Comparison of variant frequency between Japanese esophageal squamous cell carcinoma (ESCC) and The Cancer Genome Atlas (TCGA) data. Each gene is represented as a dot. The x-axis indicates the frequency in Japanese ESCC. The y-axis indicates the frequency in TCGA ESCC. The left panel indicates the frequencies of genes detected in more than 5% of our samples and TCGA ESCC. The right panel is an enlarged panel of a part of the left panel. B, Schematic of variant types and positions in NOTCH1 protein. The colors inside the square frame indicate protein motifs corresponding to a note on the bottom. The colors of the dots indicate the types of variants. Blue, missense; orange, nonsense; red, frameshift; purple, splice region. C, Effects of somatic variants in NOTCH1 and NOTCH3 on overall survival in a pooled data of our and Sawada et al.'s ESCC samples. The *P*-value was calculated by the log-rank test.



3q26.33(32%, 28/88), and 7q22.1(15%, 13/88) (Table 1). The region most frequently affected was 11q13, which was observed in approximately half of our ESCC cases and contains *CCND1*, which has been reported to be amplified in many types of cancer. In addition to the above, 8q24.21 and 3q26.33, respectively, contain *MYC* and *SOX2*, which have also been reported to be frequently amplified in many cancers, including ESCC.⁴⁻⁶ Copy number loss was frequently found at 9p21.3(34%, 30/88), where *CDKN2A* and *CDKN2B* genes locate, which has been previously reported in Japanese ESCC samples⁷ (Table 2). Loss of heterozygosity (LOH) variants were identified using VarScan, and we found that the RTK/PI3K pathway and NOTCH pathways, where NSVs were frequently detected, had variants with LOH, which were also similar to the previous study.⁷ The details of identified variants with LOH were provided in Table S4.

3.2 | Notch family somatic variants in ESCC

To examine the difference in NSV frequencies between Japanese and non-Japanese ESCCs, we compared our results with TCGA esophageal cancer data. The TCGA database provided data of 95 cases of ESCC. The somatic variant frequencies of each gene in ESCC are shown in Figure 2A. Mutated genes previously reported in ESCC, such as *TP53*, *NOTCH1*, *PIK3CA*, and *NFE2L2*, were also detected in our cases.

Among them, we focused on *NOTCH1* whose variants were detected frequently both in our ESCC cases and in TCGA ESCC cases. All amino acid alterations in *NOTCH1* were localized in the N-terminal side of the transactivating domain, and 70% of alterations (12/17) were missense (Figure 2A). In other NOTCH family genes, *NOTCH2*, *NOTCH3*, and *NOTCH4*, the amino acid alterations were identified without location bias (Figure S1a). We evaluated the effects of *NOTCH1* variants on overall survival. There was, however, no significant correlation (Figure S1b). To compare with other cohorts, we performed the log-rank test using individual ESCC patient data obtained from Sawada et al.'s study⁷ (N = 144) and TCGA (N = 94), but no similar trends were found among these three groups (Table S5). To improve statistical power by increasing sample size, we performed a pooled analysis^{18,19} using our and Sawada et al.'s Japanese ESCC samples. The Kaplan-Meier plot of *NOTCH1* was similar to the result using only TMDU-JFCR cases, although not significantly ($P = .4$), and we found that the cases with *NOTCH3* variants (N = 18) had a significantly ($P = .02$) worse prognosis than those without variants (N = 214) (Figure 2C). The results of the log-rank test of all genes using TMDU-JFCR and Sawada et al.'s samples are provided in Table S6.

3.3 | Mutational signature analysis of Japanese ESCC

Base substitution patterns of somatic variants (mutational signature) are considered to reflect tumor types or exogenous or endogenous mutagen exposure.²⁰ Therefore, we analyzed mutational signatures using 12 415 SNVs (including synonymous SNVs) detected in 88 Japanese ESCC cases. As a result, 44% (5510 SNVs) of SNVs were C>T transitions. In addition, C>G transversions flanked by a 5' thymine and any 3' nucleotide (TCN>TGN) were identified frequently (1611 SNVs, 13%).

To classify our cases by mutational signatures, we performed cluster analysis using substitution patterns of each ESCC. The samples were clustered into two distinct groups (Figure 3A). The mutation spectra of each cluster obtained by cluster analysis are shown in Figure 3B. The cluster 1 spectrum exhibited an APOBEC-associated signature, and the cluster 2 spectrum corresponded to the age-related COSMIC signature 1.²⁰

Furthermore, we evaluated the correlation between mutational signature and overall survival. Although not significant ($P = .1$), the cases with an APOBEC-associated signature (N = 37) had a slightly better prognosis than those without an APOBEC-associated signature (N = 51) (Figure 3C).

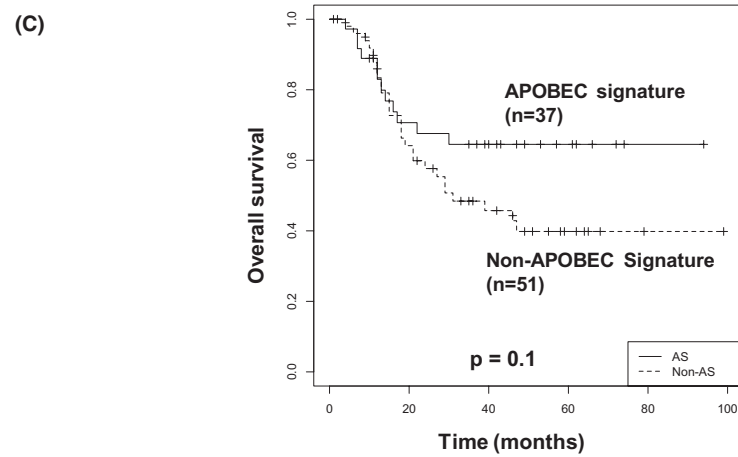
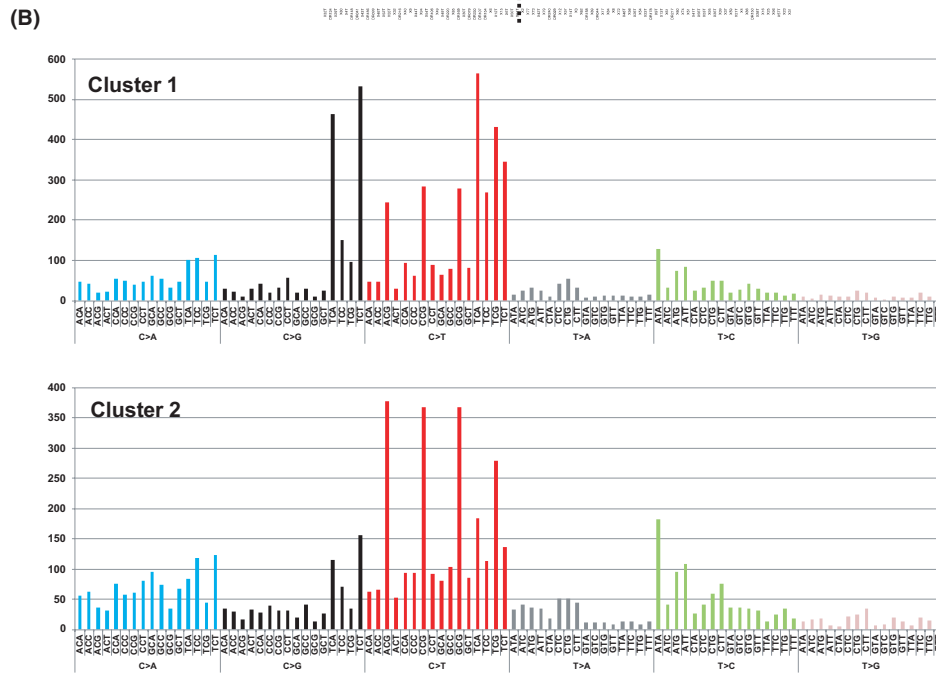
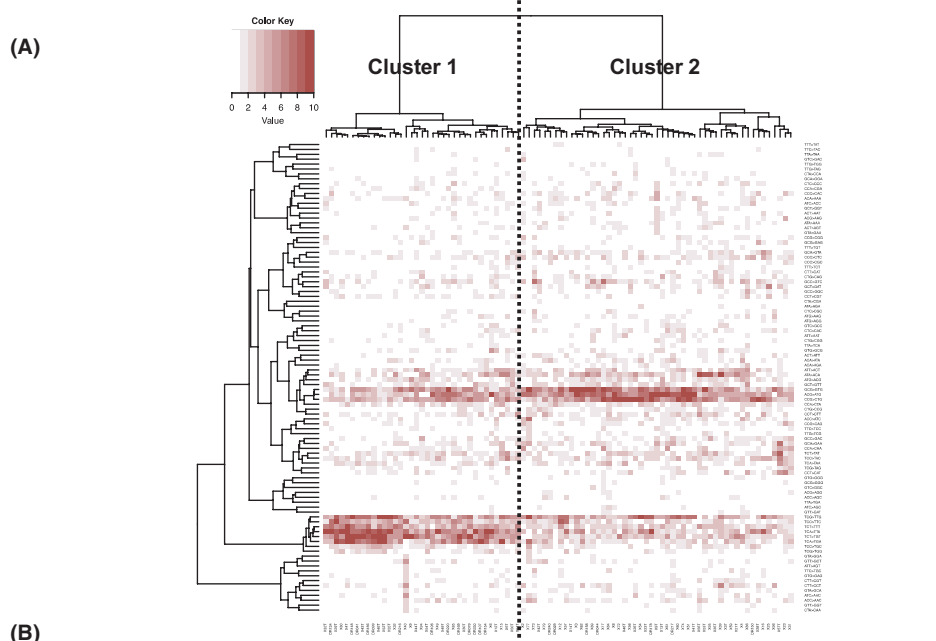
3.4 | DNA methylation profile and its correlation with gene expression of imprinted genes

Alterations of the DNA methylation status of human imprinted genes have been implicated in tumorigenesis. To clarify the DNA methylation profile and its correlation with gene expression of human imprinted genes in ESCC, we analyzed epigenomic and transcriptomic profiles integratively.

We previously reported the genome-wide DNA methylation analysis of 67 Japanese ESCC cases using Illumina Infinium HumanMethylation450 BeadChip (HM450) to explore lymph node metastasis biomarkers in ESCC.¹¹ First, we reanalyzed the DNA methylation data by the procedures described in Materials and Methods. As a result, the average numbers of hyper- and hypomethylated CpG sites were 2122 (range 46-13 557) and 2468 (range 38-16 248), respectively. The details of CpG sites used in this study are provided in Table S7.

We further examined the degree of DNA methylation alteration of imprinted genes by the procedures described in Materials and Methods, and the results are shown in Figure 4. Among a total of 1572 CpG sites in 87 imprinted genes, 63% (998/1572) of CpG sites in promoter regions were significantly hyper- or hypomethylated in tumor

FIGURE 3 Mutational signature analysis in Japanese esophageal squamous cell carcinoma (ESCC). A, Clustering heat map of substitution patterns. Each row represents a substitution pattern. Substitution patterns are divided into 96 patterns defined by the substituted base with flanking 5' and 3' nucleotides. Each column represents an individual sample. Color density is proportional to the frequency of substitution patterns. B, Mutation spectra of each cluster divided by clustering analysis. The x-axis indicates 96 substitution patterns. The y-axis indicates the number of CpG sites. C, Effects of an APOBEC-associated signature on overall survival. Samples with an APOBEC-associated signature correspond to cluster 1. The P -value was calculated by the log-rank test.



samples compared with paired nontumor samples (q -values ≤ 0.05 , Wilcoxon signed-rank test). In order to compare other functions or pathways, 912 gene sets extracted from MSigDB HALLMARK,²¹ KEGG,²²⁻²⁴ REACTOME,^{25,26} and COSMIC²⁷ databases were evaluated by the same procedure, revealing human imprinted genes to be highly altered (q -value = 7.76×10^9 , hypergeometric distribution) (Figure 4B,C). The results of the top 50 and all gene sets are listed in Table 3 and Table S8, respectively.

In individual patients, hyper- or hypomethylated CpG sites were enriched in imprinted genes compared with tumor suppressor genes, such as *APC*, *CDH1*, and *CDKN2A*, which are well known to be involved in aberrant DNA methylation in tumors, including ESCC²¹ (Figure 4D). The heatmaps of DNA methylation alteration also demonstrated a significant difference in methylation status of imprinted genes compared with tumor suppressor genes (Figure 4E,F).

Next, we examined the correlations between delta-beta values and gene expression changes between 57 paired tumors and nontumor samples with both HM450 and RNA-seq data. The details of expression fold changes for all genes are provided in Table S9. In imprinted genes, 6.5% of CpG sites were negatively correlated (Pearson correlation coefficient $\leq -.3$) between delta-beta values and gene expression fold changes, which were higher in the gene sets with more DNA methylation alterations, suggesting that DNA methylation changes affect gene expression (Table 3). CpG probe ID cg04029027 located in the promoter region of *MEST* (*PEG1*), a well-known imprinted gene, exhibited a significant negative correlation between DNA methylation and gene expression (Pearson correlation coefficient = $-.55$) (Figure 4G). Another example of an imprinted gene, *BLCAP*, is shown in Figure 4H. CpG probe ID cg21733794 located in the promoter region of *BLCAP* demonstrated a similar significant negative correlation (Pearson correlation coefficient = $-.67$).

3.5 | Analysis of AEI in Japanese ESCC

In previous studies, several cancer related genes were found to be involved in AEIs not only in lung, breast, and liver cancers²²⁻²⁴ but

also in several cancer cell lines.^{25,26} However, the genome-wide profiles of AEIs remain unclear in Japanese ESCC. We analyzed AEIs using the data from 56 ESCC cases in a Japanese population as described in the Materials and Methods section. In this study, nonsynonymous AEI genes were defined as genes whose transcripts were predominantly expressed from only one allele harboring nonsynonymous variants and little from the paired allele, and a total of 1567 AEI genes (range 0-104/cases) were identified, of which 1015 were nonsynonymous AEI genes (Figure 5A). Frequently detected nonsynonymous AEI genes are listed in Table 4.

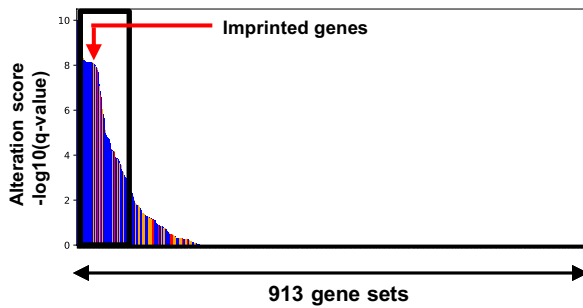
Of these, we focused on FAT family genes because several mutations have been reported in ESCC.^{5,6} AEIs and SNVs of *FAT1* and *FAT2* genes were detected without hot-spot regions (Figure 5B). One ESCC example, sample ID 49, in which AEI occurred in *FAT2*, is shown in Figure 5C. Of 10 AEI variants supporting the existence of AEI in *FAT2* in this case, four representative genomic positions (chr5: 150930345, 150925728, 150924769, and 150901261) are shown. WES data demonstrated that both alleles existed in tumor and nontumor tissues, suggesting no somatic variant at the genomic position. However, *FAT2* was transcribed from only one allele harboring a nonsynonymous variant in the tumor even though *FAT2* was transcribed from both alleles in nontumor tissues. Of note, based on HM450 data obtained in our previous study,²⁷ methylation levels of CpGs located in the *FAT2* promoter region differed little between tumor and nontumor tissues (Table S10), suggesting that allelic loss or DNA hypermethylations in promoter regions did not cause AEI, although the mechanism of AEI of *FAT2* has not been clarified. In addition, 32% (18/56) of ESCC cases with nonsynonymous SNVs or AEI in FAT family genes tended to be detected in a mutually exclusive manner, although not significantly, particularly between *FAT1* and *FAT2* (Figure 5D). Our study using the combination of WES and RNA-seq revealed the skewed allelic expression of FAT family genes involved in their genetic variants causing amino acid alterations. The details of identified AEI positions were provided in Table S11.

FIGURE 4 DNA methylation status of imprinted genes and its correlation with gene expression. A, A scheme for the evaluation of DNA methylation alterations. DNA methylation alteration of each GpG site between tumors and paired nontumors was assessed using the Wilcoxon signed-rank test. CpG sites with q -values < 0.05 were treated as significantly altered CpG sites. Enrichment of significant CpG sites in a gene set was tested using hypergeometric distribution. The gene sets with q -values < 0.05 were treated as DNA methylation-enriched gene sets. Alteration scores = $-\log_{10}(q\text{-values})$. Correlations between delta-beta and gene expression fold change from RNA sequencing (RNA-seq) were assessed using Pearson correlation coefficients. Pat, patient; NS, not significant. B, Alteration scores of 913 gene sets including imprinted genes. The bar color indicates the degree of correlation between delta-beta and gene expression fold change. Red, more than 10% of CpG sites are negatively correlated (Pearson correlation coefficient $\leq -.3$); orange, more than 5% of CpG sites are negatively correlated; blue; $< 5\%$ of CpG sites are negatively correlated. C, Alteration scores of the top 100 gene sets. D, Methylation status changes of individual patients in imprinted genes and tumor suppressor genes. Each dot indicates an individual patient. The y-axis indicates the percentage of hyper- or hypomethylated CpG sites. Blue; hypermethylated; orange, hypomethylated. E, Clustering heat map of CpG sites in imprinted genes. Red, sky blue, and gray indicate hypermethylation (delta-beta > 0), hypomethylation (delta-beta < 0), and no change, respectively. Color density is proportional to the delta-beta values. Each row indicates a CpG site, and each column indicates an individual sample. F, Clustering heat map of CpG sites in tumor suppressor genes. G, Correlation between delta-beta of CpG site cg04029027 and gene expression in *MEST* (*PEG1*). The x-axis and y-axis indicate delta-beta in HM450 and fold change (\log_2) in RNA-seq, respectively. Each sample is represented as a dot. The P -value was calculated by the test for noncorrelation. H, Correlation between delta-beta of CpG site cg21733794 and gene expression in *BLCAP*

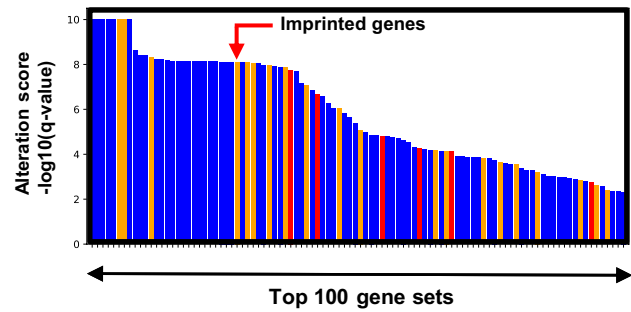
(A)

	CpG site	Methylation status								Wilcoxon signed-rank test	Alteration score	Gene expression	
		Tumor				Non-Tumor						Correlation between Methylation and Gene expression	Bar color
		Pat. 1	Pat. 2	...	Pat. N	Pat. 1	Pat. 2	...	Pat. N				
Geneset A	CpG 1	0.8	0.7	...	0.6	0.2	0.1	...	0.3	Significant	8.5	-0.5	correlated CpG sites
	CpG 2	0.2	0.1	...	0.3	0.2	0.1	...	0.3	NS		0.2	
	CpG N	0.8	0.7	...	0.6	0.2	0.1	...	0.3	Significant		-0.6	
Geneset B	CpG 1	0.2	0.1	...	0.3	0.2	0.1	...	0.3	Significant	0.1	-0.4	red >= 10% orange >= 5% blue < 5%
	CpG 2	0.2	0.1	...	0.3	0.2	0.1	...	0.3	NS		0.3	
	CpG N	0.8	0.7	...	0.6	0.7	0.6	...	0.6	NS		0.5	

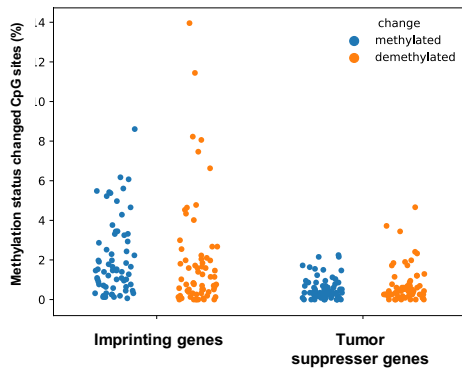
(B)



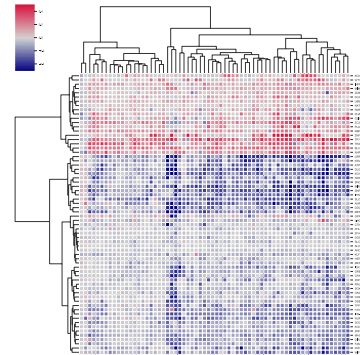
(C)



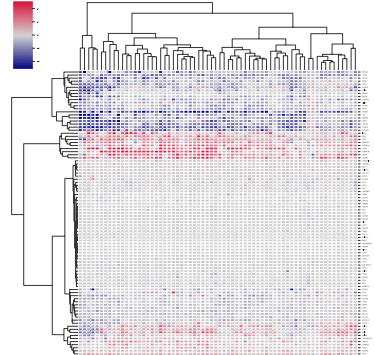
(D)



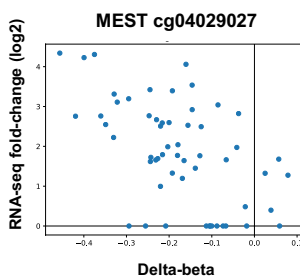
(E)



(F)



(G)



(H)

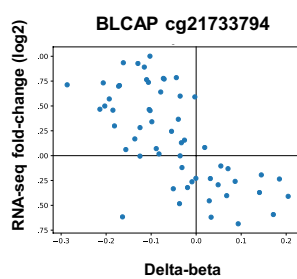


TABLE 3 Top 50 gene sets significantly enriched in DNA methylation alterations

Database	Gene set	Genes in gene set	CpG sites in gene set	Significant CpG sites in gene set	P-value	q-value	Methylation-expression-correlated CpGs (%)
REACTOME	SIGNALING-BY-GPCR	829	4685	2814	0	0	2.6
KEGG	OLFACTORY-TRANSDUCTION	320	887	751	0	0	0.6
KEGG	CYTOKINE-CYTOKINE-RECEPTOR-INTERACTION	244	1327	792	0	0	3.3
REACTOME	NEURONAL-SYSTEM	274	2249	1227	0	0	2.4
REACTOME	PEPTIDE-LIGAND-BINDING-RECEPTORS	181	1100	743	0	0	2.6
KEGG	HEMATOPOIETIC-CELL-LINEAGE	82	443	279	0	0	6.3
KEGG	AUTOIMMUNE-THYROID-DISEASE	39	241	158	0	0	5.4
REACTOME	GABA-A-RECEPTOR-ACTIVATION	12	131	99	0	0	0.0
REACTOME	G-ALPHA-S-SIGNALLING-EVENTS	117	932	515	2.34E-11	2.38E-09	2.5
REACTOME	SEROTONIN-RECEPTORS	12	87	72	4.67E-11	4.06E-09	0.0
REACTOME	DEFENSINS	39	126	114	4.90E-11	4.06E-09	0.7
REACTOME	IMMUNOREGULATORY-INTERACTIONS-BETWEEN-A-LYMPHOID-AND-A-NON-LYMPHOID-CELL	60	389	259	6.62E-11	5.04E-09	7.9
REACTOME	NEUROTRANSMITTER-RECEPTOR-BINDING-AND-DOWNSTREAM-TRANSMISSION-IN-THE-POSTSYNAPTIC-CELL	133	1062	594	9.14E-11	6.22E-09	2.5
REACTOME	GPCR-LIGAND-BINDING	388	2599	1590	9.54E-11	6.22E-09	2.9
KEGG	ASTHMA	28	150	112	1.12E-10	6.83E-09	4.0
REACTOME	CLASS-A1-RHODOPSIN-LIKE-RECEPTORS	289	1760	1160	1.30E-10	7.17E-09	2.8
REACTOME	AMINE-DERIVED-HORMONES	14	103	80	1.35E-10	7.17E-09	0.0
REACTOME	LIGAND-GATED-ION-CHANNEL-TRANSPORT	21	197	140	1.56E-10	7.17E-09	0.0
REACTOME	TRANSLOCATION-OF-ZAP-70-TO-IMMUNOLOGICAL-SYNAPSE	13	65	56	1.67E-10	7.17E-09	2.9
KEGG	NEUROACTIVE-LIGAND-RECEPTOR-INTERACTION	265	1817	1175	1.67E-10	7.17E-09	1.9
REACTOME	AMINE-LIGAND-BINDING-RECEPTORS	36	247	169	1.72E-10	7.17E-09	0.8
REACTOME	G-ALPHA-I-SIGNALLING-EVENTS	187	1296	765	1.73E-10	7.17E-09	3.0
REACTOME	GPCR-DOWNSTREAM-SIGNALING	721	3876	2456	1.95E-10	7.51E-09	2.4

(Continues)

TABLE 3 (Continued)

Database	Gene set	Genes in gene set	CpG sites in gene set	Significant CpG sites in gene set	P-value	q-value	Methylation-expression-correlated CpGs (%)
REACTOME	TRANSMISSION-ACROSS-CHEMICAL-SYNAPSES	182	1508	817	1.97E-10	7.51E-09	2.4
REACTOME	BETA-DEFENSINS	31	101	92	2.16E-10	7.76E-09	0.0
REACTOME	ION-CHANNEL-TRANSPORT	54	421	258	2.28E-10	7.76E-09	4.3
REACTOME	G-ALPHA-Q-SIGNALLING-EVENTS	175	1189	699	2.37E-10	7.76E-09	4.5
Babak et al. <i>Nat. Genet.</i>	Imprinted genes	87	1572	998	2.38E-10	7.76E-09	6.5
REACTOME	GASTRIN-CREB-SIGNALLING-PATHWAY-VIA-PKC-AND-MAPK	196	1356	760	2.65E-10	8.33E-09	4.5
KEGG	GRAFT-VERSUS-HOST-DISEASE	37	235	166	2.76E-10	8.41E-09	5.5
KEGG	ALLOGRAFT-REJECTION	35	238	155	3.22E-10	9.30E-09	5.4
REACTOME	OLFACTORY-SIGNALING-PATHWAY	264	647	616	3.26E-10	9.30E-09	0.0
KEGG	TYPE-I-DIABETES-MELLITUS	41	309	195	3.80E-10	1.05E-08	4.2
HALLMARK	KRAS-SIGNALING-DN	197	1394	786	4.13E-10	1.11E-08	5.2
REACTOME	CHEMOKINE-RECEPTORS-BIND-CHEMOKINES	53	267	186	4.57E-10	1.19E-08	3.0
REACTOME	POTASSIUM-CHANNELS	98	805	451	5.13E-10	1.30E-08	2.5
KEGG	CELL-ADHESION-MOLECULES-CAMS	130	912	504	5.75E-10	1.42E-08	6.2
REACTOME	GAP-JUNCTION-ASSEMBLY	18	148	104	7.38E-10	1.77E-08	18.9
KEGG	COMPLEMENT-AND-COAGULATION-CASCADES	68	327	202	9.00E-10	2.11E-08	4.0
REACTOME	ORGANIC-CATION-ANION-ZWITTERION-TRANSPORT	13	112	81	3.06E-09	6.98E-08	0.9
HALLMARK	ALLOGRAFT-REJECTION	197	1411	740	4.00E-09	8.91E-08	7.2
REACTOME	INCRETIN-SYNTHESIS-SECRETION-AND-INACTIVATION	21	162	109	6.56E-09	1.43E-07	0.6
KEGG	DRUG-METABOLISM-CYTOCHROME-P450	67	334	201	1.06E-08	2.26E-07	15.4
REACTOME	O-LINKED-GLYCOSYLATION-OF-MUCINS	53	346	207	1.28E-08	2.66E-07	3.5
KEGG	INTESTINAL-IMMUNE-NETWORK-FOR-IGA-PRODUCTION	46	276	169	2.81E-08	5.71E-07	4.3
REACTOME	GABA-RECEPTOR-ACTIVATION	52	455	261	4.59E-08	9.03E-07	2.0

(Continues)

TABLE 3 (Continued)

Database	Gene set	Genes in gene set	CpG sites in gene set	Significant CpG sites in gene set	P-value	q-value	Methylation-expression-correlated CpGs (%)
KEGG	STEROID-HORMONE-BIOSYNTHESIS	51	304	183	4.65E-08	9.03E-07	6.2
REACTOME	GENERATION-OF-SECOND-MESSENGER-MOLECULES	26	133	90	8.37E-08	1.59E-06	2.2
REACTOME	COMPLEMENT-CASCADE	28	116	80	1.23E-07	2.29E-06	0.9
REACTOME	PHOSPHORYLATION-OF-CD3-AND-TCR-ZETA-CHAINS	15	64	49	2.24E-07	4.09E-06	2.9

TABLE 4 Frequently identified nonsynonymous allelic expression imbalance (AEI) genes

Gene	Location	Number of samples
TNC	9q33.1	14
SERPINB5	18q21.33	11
CTNNAL1	9q31.3	8
KIAA0368	9q31.3	8
FAT2	5q33.1	8
TBC1D2	9q22.33	7
AHNAK2	14q32.33	7
HGS	17q25.3	7
MAP3K1	5q11.2	7
SETX	9q34.13	7
SVIL	10p11.23	7
SPINK5	5q32	7
KANK1	9p24.3	6
TMEM245	9q31.3	6
LRRFIP1	2q37.3	5
FRMD4B	3p14.1	5
CDH3	16q22.1	5
PSMB6	17p13.2	5
PI4K2B	4p15.2	5
PSD3	8p22	5
PDCD6IP	3p22.3	5
PTPN13	4q21.3	5
IKBKAP	9q31.3	5
UBP1	3p22.3	5
FAT1	4q35.2	5
PTBP3	9q32	5
DSC3	18q12.1	5
GNL3	3p21.1	5
MKI67	10q26.2	5
CCDC137	17q25.3	5
ITGB4	17q25.1	5

4 | Discussion

In this study, we revealed the landscape of genomic, DNA-methylation, and gene-expression profiles in ESCCs in a Japanese population by omics analyses. In WES analysis, SNVs and focal amplification in the RTK/PI3K pathway, NOTCH family, and NFE2L2 pathway were detected in a mutually exclusive manner in our ESCC cases. The TCGA Research Network demonstrated that most ESCC cases are classified into two subtypes by multi-omics profiles: One is characterized by mutations in the NFE2L2 pathway and the other is characterized by mutation of *NOTCH1* or *ZNF750*.⁴ This report is consistent with our study. Moreover, our study suggested the existence of a subtype characterized by genomic alterations in RTK/PI3K pathway genes in addition to the two subtypes mentioned above.

We found that 26% (23/88) of ESCC cases harbored somatic variants in NOTCH family genes, similar to previous reports.⁴⁻⁷ The effects of *NOTCH1* variants are context dependent. For example, *NOTCH1* variants in the hematopoietic system are frequently detected on the C-terminal PEST domain and are considered to be gain-of-function.²⁸⁻³⁰ On the other hand, *NOTCH1* variants in several solid tumors are loss-of-function.³¹⁻³⁴ Consequently, the variants we identified in our ESCC cases are probably loss-of-function variants. ESCC caused by the lack of NOTCH functions may be less malignant than ESCC caused by other factors because the cases with *NOTCH1* variants had a better prognosis than those without *NOTCH1* variants, although not significantly (Figure 2C). Indeed, a recently published study found a marked overrepresentation of *NOTCH1* mutations in physiologically normal esophageal epithelia compared with ESCC.³⁵ The presence of *NOTCH1* variants can accelerate carcinogenesis, but the correlation between ESCC malignancy and presence of *NOTCH1* variants remains unclear. Furthermore, the cases with *NOTCH3* variants had a significantly worse prognosis than those without variants (Figure 2C). Although the relevance between *NOTCH3* variants and prognosis is still unknown, it has been reported that *NOTCH3* downregulation decreases chemotherapy sensitivity through activation of epithelial-mesenchymal transition (EMT), which may lead to worsening prognosis.³⁶ Considering that numerous mutations

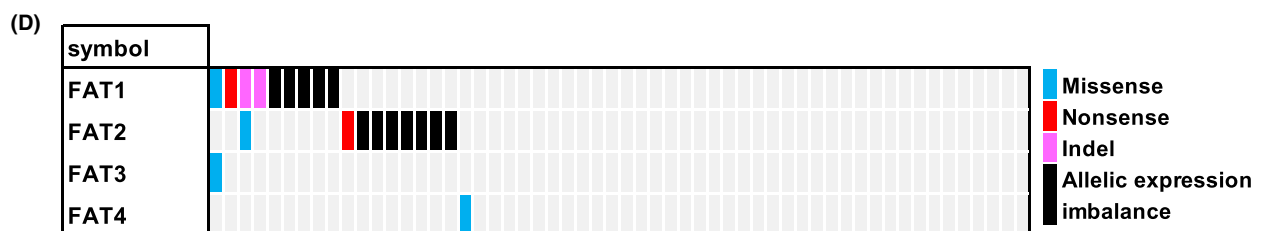
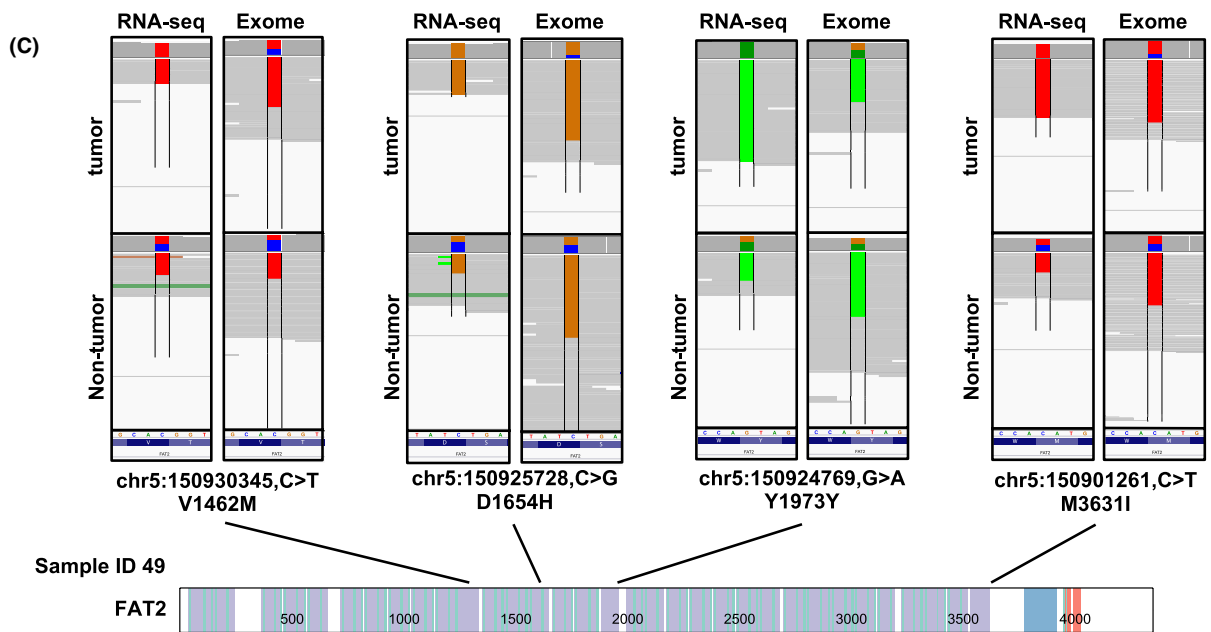
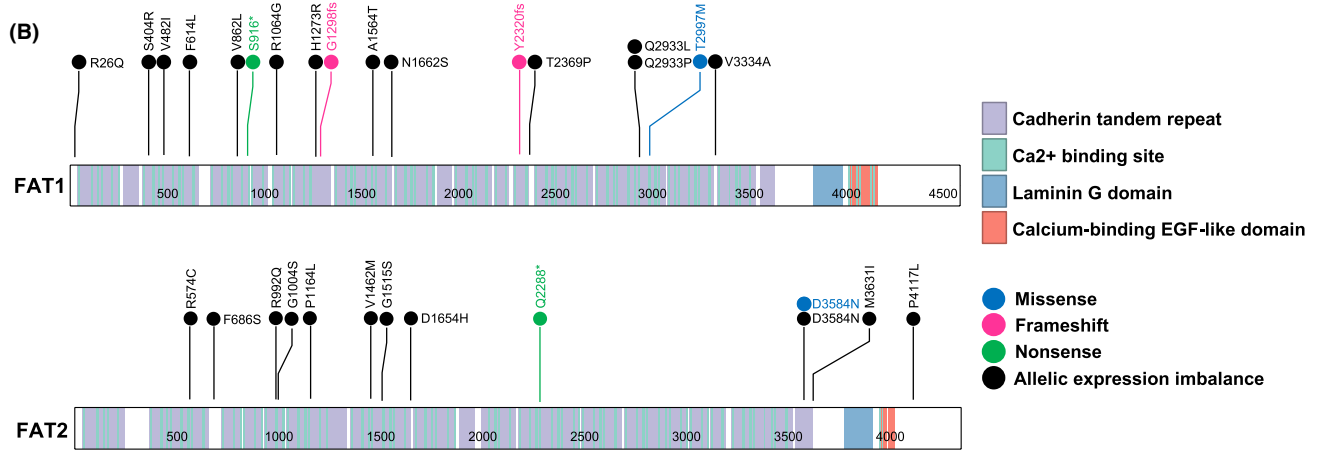
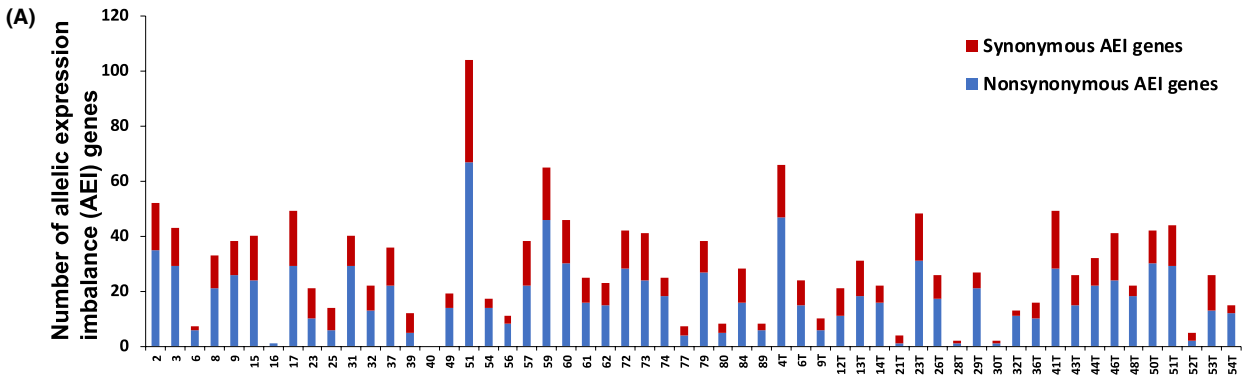


FIGURE 5 Analysis of allelic expression imbalance (AEI). A, The number of genes with AEI (vertical axis) in each sample (horizontal axis). The blue bar represents nonsynonymous AEI genes, which express transcripts with predominantly amino acid alterations. The red bar represents synonymous AEI genes without subsequent amino acid alterations. B, Schematics of amino acid alterations caused by SNVs and AEI in *FAT1* and *FAT2* proteins. The colors inside the square frame indicate protein motifs corresponding to a note on the right side. The colors of the dots indicate the types of amino acid changes caused by somatic variants or AEI. Blue, missense; red, frameshift; green, nonsense; black, AEI. C, RNA sequencing (RNA-seq) and WES data of *FAT2* nucleotide alterations suggested AEI in a Japanese esophageal squamous cell carcinoma (ESCC) patient (sample ID 49) visualized by integrative genomics viewer (IGV). The gray area indicates aligned sequence reads and the horizontal axis indicates genomic coordinates. Other colors indicate nucleotides differing from reference sequences. Red, thymine; brown, guanine; green, adenine; blue, cytosine. D, The matrix of detected variants and nonsynonymous AEI in *FAT* family genes [Correction added on 19 August 2021, after first online publication: Figure 5C has been corrected.]

in NOTCH family in solid tumors have been reported as loss-of-function,³¹⁻³⁴ we think our result supports these findings.

Approximately half of our ESCC cases had an APOBEC-associated mutational signature, consistent with previous studies.^{7,8} However, nonsynonymous variants in APOBEC1 were detected in only two cases, and no variants in other APOBEC family genes were detected in our ESCC cases. Roberts et al. reported that an APOBEC-associated mutational signature is correlated with APOBEC mRNA levels; however, the association was relatively low, so they suggested that other factors play a role in an APOBEC-associated mutational signature.³⁷ In our ESCC cases, we found no significant correlations between an APOBEC-associated mutational signature and mRNA expression levels of APOBEC family genes (Figure S2). Further analysis is required to identify factors causing an APOBEC-associated mutational signature.

We demonstrated that the profiles of DNA methylation and gene expression are aberrant in imprinted genes in ESCCs. Although loss of imprinting (LOI) of imprinted genes was previously reported in cancer,³⁸⁻⁴⁰ we newly identified that the aberration levels of DNA methylation and gene expression are higher across the imprinted genes than in other gene sets in ESCCs. In particular, LOI of *MEST* (*PEG1*) has been reported in breast cancer⁴¹ and lung cancer cell lines,⁴² and our study demonstrated LOI of *MEST* in our ESCC cases. Although we were unable to detect alteration of AEI status in *MEST* due to limitations of AEI analysis using RNA-seq data, LOI and skewed allelic expression of the *MEST* gene may play important roles in ESCC tumorigenesis.

Although AEI has been reported in several cancer-related genes, few genome-wide analyses of AEI in cancer have been reported. As RNA-seq analysis can widely detect AEI genes, we performed genome-wide AEI analysis of ESCCs in Japanese patients. As a result, 21% (12/56) of ESCC tumors had allele-specific transcripts in *FAT1* and *FAT2* genes. The AEI of *FAT* family genes has not been reported in ESCC, although *FAT2* AEI was reported in oral squamous cell carcinoma⁴³ and Lin et al. previously reported that ESCC frequently harbors exclusive truncations in *FAT1*, *FAT2*, and *FAT3* in a mutually exclusive manner.⁵ One possible cause of AEI is LOH. Indeed, frequent LOH of the *FAT1* locus was reported previously in astrocytic tumors.⁴⁴ However, all ESCCs with AEI in *FAT1* or *FAT2* had no LOH in these loci because sequence reads of these samples by WES suggested the existence of both alleles (Figure 5B and Figure S3). Furthermore, silencing of *FAT1* or *FAT2* genes due to DNA methylation was not detected except

in one case (Table S10), suggesting that AEI genes are induced in an epigenetic manner, including histone modification other than DNA methylation in the ESCCs we analyzed. Indeed, Inoue et al. reported that DNA methylation-independent allele-specific expression is caused by maternal histone H3K27 trimethylation in mice.⁴⁵ Further exploration, including histone modification analysis, is required to elucidate the mechanism of AEI involved in *FAT1* and *FAT2* in ESCCs.

FAT family genes encode transmembrane proteins and members of the cadherin superfamily. It is generally assumed that *FAT* family genes are tumor suppressor genes.⁴⁶ Several nonsynonymous variants in *FAT* family genes were previously reported, and most of them are loss-of-function variants.^{5,47} Thus, nonsynonymous AEI of *FAT* family genes identified in this study may result in functional loss of these genes, which leading to ESCC tumorigenesis. RNA-seq analysis enabled us to detect nonsynonymous AEI of *FAT* family genes in 21% (12/56) of our ESCC cases. On the other hand, WES detected SNVs only in 10% (6/56). However, the correlation between variants or AEI in *FAT* family genes and clinical information has not been clarified (Figure S4). The combination of WES and RNA-seq analyses is required to identify the precise functional status of *FAT* family genes.

In this study, we performed integrative genome, DNA-methylation, and gene expression analyses, and identified the landscape of genome and epigenome profiles in Japanese ESCCs. Integrative analysis of multiomics data is a powerful tool for genome medicine and cancer biology.

Acknowledgments

The authors thank Ayako Takahashi and Rumi Mori (Tokyo Medical and Dental University, Japan) for their technical assistance.

DISCLOSURE

The authors declare no conflict of interest.

Authors' Contribution

A.T., K.T., Ju.I., T.N., and J.I. contributed to the conception and design of the study. A.T., K.T., and S.M. contributed to DNA sequencing of tumor samples. A.T., K.T., and J.I. contributed to the acquisition and interpretation of data. A.T., N.F., and S.M. contributed to sampling of tumor specimens. A.T. provided information for clinical implication. A.T., K.T., and J.I. wrote the manuscript. All authors read and approved the final manuscript.

ORCID

Kousuke Tanimoto  <https://orcid.org/0000-0002-0826-2940>

Johji Inazawa  <https://orcid.org/0000-0002-3945-2800>

REFERENCES

1. Ferlay J, Shin HR, Bray F, Forman D, Mathers C, Parkin DM. Estimates of worldwide burden of cancer in 2008: GLOBOCAN 2008. *Int J Cancer*. 2010;127:2893–2917.
2. Lin Y, Totsuka Y, He Y, et al. Epidemiology of esophageal cancer in Japan and China. *J Epidemiol*. 2013;23:233–242.
3. Pennathur A, Gibson MK, Jobe BA, Luketich JD. Oesophageal carcinoma. *Lancet*. 2013;381:400–412.
4. Network CGAR, University AWGA, Agency BC, et al. Integrated genomic characterization of oesophageal carcinoma. *Nature*. 2017;541:169–175.
5. Lin DC, Hao JJ, Nagata Y, et al. Genomic and molecular characterization of esophageal squamous cell carcinoma. *Nat Genet*. 2014;46:467–473.
6. Gao YB, Chen ZL, Li JG, et al. Genetic landscape of esophageal squamous cell carcinoma. *Nat Genet*. 2014;46:1097–1102.
7. Sawada G, Niida A, Uchi R, et al. genomic landscape of esophageal squamous cell carcinoma in a Japanese population. *Gastroenterology*. 2016;150:1171–1182.
8. Zhang L, Zhou Y, Cheng C, et al. Genomic analyses reveal mutational signatures and frequently altered genes in esophageal squamous cell carcinoma. *Am J Hum Genet*. 2015;96:597–611.
9. Song Y, Li L, Ou Y, et al. Identification of genomic alterations in oesophageal squamous cell cancer. *Nature*. 2014;509:91–95.
10. Dutta M, Nakagawa H, Kato H, et al. Whole genome sequencing analysis identifies recurrent structural alterations in esophageal squamous cell carcinoma. *PeerJ*. 2020;8:e9294.
11. Nagata H, Kozaki KI, Muramatsu T, et al. Genome-wide screening of DNA methylation associated with lymph node metastasis in esophageal squamous cell carcinoma. *Oncotarget*. 2017;8:37740–37750.
12. Babak T, DeVeale B, Tsang EK, et al. Genetic conflict reflected in tissue-specific maps of genomic imprinting in human and mouse. *Nat Genet*. 2015;47:544–549.
13. McKenna A, Hanna M, Banks E, et al. The Genome Analysis Toolkit: a MapReduce framework for analyzing next-generation DNA sequencing data. *Genome Res*. 2010;20:1297–1303.
14. Zhou X, Edmonson MN, Wilkinson MR, et al. Exploring genomic alteration in pediatric cancer using ProteinPaint. *Nat Genet*. 2016;48:4–6.
15. Robinson JT, Thorvaldsdóttir H, Winckler W, et al. Integrative genomics viewer. *Nat Biotechnol*. 2011;29:24–26.
16. Thorvaldsdóttir H, Robinson JT, Mesirov JP. Integrative Genomics Viewer (IGV): high-performance genomics data visualization and exploration. *Brief Bioinform*. 2013;14:178–192.
17. Robinson JT, Thorvaldsdóttir H, Wenger AM, Zehir A, Mesirov JP. Variant review with the integrative genomics viewer. *Cancer Res*. 2017;77:e31–e34.
18. Cholesterol, diastolic blood pressure, and stroke: 13,000 strokes in 450,000 people in 45 prospective cohorts. Prospective studies collaboration. *Lancet*. 1995;346:1647–1653.
19. Friedenreich CM. Commentary: improving pooled analyses in epidemiology. *Int J Epidemiol*. 2002;31:86–87.
20. Alexandrov LB, Nik-Zainal S, Wedge DC, et al. Signatures of mutational processes in human cancer. *Nature*. 2013;500:415–421.
21. Baba Y, Watanabe M, Baba H. Review of the alterations in DNA methylation in esophageal squamous cell carcinoma. *Surg Today*. 2013;43:1355–1364.
22. Nomoto S, Haruki N, Kondo M, Konishi H, Takahashi T. Search for mutations and examination of allelic expression imbalance of the p73 gene at 1p36.33 in human lung cancers. *Cancer Res*. 1998;58:1380–1383.
23. Chen X, Weaver J, Bove BA, et al. Allelic imbalance in BRCA1 and BRCA2 gene expression is associated with an increased breast cancer risk. *Hum Mol Genet*. 2008;17:1336–1348.
24. Aihara T, Noguchi S, Miyoshi Y, et al. Allelic imbalance of insulin-like growth factor II gene expression in cancerous and precancerous lesions of the liver. *Hepatology*. 1998;28:86–89.
25. Hosokawa Y, Arnold A. Mechanism of cyclin D1 (CCND1, PRAD1) overexpression in human cancer cells: analysis of allele-specific expression. *Genes Chromosomes Cancer*. 1998;22:66–71.
26. Milani L, Gupta M, Andersen M, et al. Allelic imbalance in gene expression as a guide to cis-acting regulatory single nucleotide polymorphisms in cancer cells. *Nucleic Acids Res*. 2007;35:e34.
27. Nagata H, Kozaki KI, Muramatsu T, et al. Genome-wide screening of DNA methylation associated with lymph node metastasis in esophageal squamous cell carcinoma. *Oncotarget*. 2017;8(23):37740–37750.
28. Love C, Sun Z, Jima D, et al. The genetic landscape of mutations in Burkitt lymphoma. *Nat Genet*. 2012;44:1321–1325.
29. Weng AP, Ferrando AA, Lee W, et al. Activating mutations of NOTCH1 in human T cell acute lymphoblastic leukemia. *Science*. 2004;306:269–271.
30. Pancewicz J, Taylor JM, Datta A, et al. Notch signaling contributes to proliferation and tumor formation of human T-cell leukemia virus type 1-associated adult T-cell leukemia. *Proc Natl Acad Sci U S A*. 2010;107:16619–16624.
31. Stransky N, Egloff AM, Tward AD, et al. The mutational landscape of head and neck squamous cell carcinoma. *Science*. 2011;333:1157–1160.
32. Agrawal N, Frederick MJ, Pickering CR, et al. Exome sequencing of head and neck squamous cell carcinoma reveals inactivating mutations in NOTCH1. *Science*. 2011;333:1154–1157.
33. Wang NJ, Sanborn Z, Arnett KL, et al. Loss-of-function mutations in Notch receptors in cutaneous and lung squamous cell carcinoma. *Proc Natl Acad Sci U S A*. 2011;108:17761–17766.
34. Ntziachristos P, Lim JS, Sage J, Aifantis I. From fly wings to targeted cancer therapies: a centennial for notch signaling. *Cancer Cell*. 2014;25:318–334.
35. Yokoyama A, Kakiuchi N, Yoshizato T, et al. Age-related remodeling of oesophageal epithelia by mutated cancer drivers. *Nature*. 2019;565:312–317.
36. Matsuura N, Tanaka K, Yamasaki M, et al. NOTCH3 limits the epithelial-mesenchymal transition and predicts a favorable clinical outcome in esophageal cancer. *Cancer Med*. 2021;10:3986–3996.
37. Roberts SA, Lawrence MS, Klimczak LJ, et al. An APOBEC cytidine deaminase mutagenesis pattern is widespread in human cancers. *Nat Genet*. 2013;45:970–976.
38. Cui H, Onyango P, Brandenburg S, Wu Y, Hsieh CL, Feinberg AP. Loss of imprinting in colorectal cancer linked to hypomethylation of H19 and IGF2. *Cancer Res*. 2002;62:6442–6446.
39. Kaneda A, Wang CJ, Cheong R, et al. Enhanced sensitivity to IGF-II signaling links loss of imprinting of IGF2 to increased cell proliferation and tumor risk. *Proc Natl Acad Sci U S A*. 2007;104:20926–20931.
40. Zhao R, DeCoteau JF, Geyer CR, Gao M, Cui H, Casson AG. Loss of imprinting of the insulin-like growth factor II (IGF2) gene in esophageal normal and adenocarcinoma tissues. *Carcinogenesis*. 2009;30:2117–2122.
41. Pedersen IS, Dervan PA, Broderick D, et al. Frequent loss of imprinting of PEG1/MEST in invasive breast cancer. *Cancer Res*. 1999;59:5449–5451.
42. Nakanishi H, Suda T, Katoh M, et al. Loss of imprinting of PEG1/MEST in lung cancer cell lines. *Oncol Rep*. 2004;12:1273–1278.

43. Tuch BB, Laborde RR, Xu X, et al. Tumor transcriptome sequencing reveals allelic expression imbalances associated with copy number alterations. *PLoS One*. 2010;5:e9317.
44. Chosdol K, Misra A, Puri S, et al. Frequent loss of heterozygosity and altered expression of the candidate tumor suppressor gene 'FAT' in human astrocytic tumors. *BMC Cancer*. 2009;9:5.
45. Inoue A, Jiang L, Lu F, Suzuki T, Zhang Y. Maternal H3K27me3 controls DNA methylation-independent imprinting. *Nature*. 2017;547:419–424.
46. Katoh M. Function and cancer genomics of FAT family genes (review). *Int J Oncol*. 2012;41:1913–1918.
47. Morris LG, Kaufman AM, Gong Y, et al. Recurrent somatic mutation of FAT1 in multiple human cancers leads to aberrant Wnt activation. *Nat Genet*. 2013;45:253–261.

SUPPORTING INFORMATION

Additional supporting information may be found online in the Supporting Information section.

How to cite this article: Takemoto A, Tanimoto K, Mori S, et al. Integrative genome-wide analyses reveal the transcriptional aberrations in Japanese esophageal squamous cell carcinoma. *Cancer Sci*. 2021;112:4377–4392. <https://doi.org/10.1111/cas.15063>